of patients most likely to benefit from expensive and difficult surveillance procedures.
Design: Non-dysplastic rectal biopsies were analyzed from 10 UC patients with synchronous but distant colon cancer (UC-progressors), 10 without dysplasia for >10 years (UC-nonprogressors), and 18 normal controls. Next generation small RNA sequencing was performed on the Illumina platform. Data were analyzed using the USeq software package to determine regions of differential expression between these patient groups. RT-PCR, in situ hybridization, and immunohistochemistry were performed for validation purposes and to identify which cells differentially express micro-RNAs within the tested biopsies.
Results: While 11 miRNAs were misregulated in both UC patient groups compared to normals, a total of 33 miRNAs were differentially expressed between progressors and nonprogressors using our statistical criteria (fold change >2, false discovery rate < 0.10). RT-PCR confirmed these RNA-sequencing results. Of particular interest, mir-155 was overexpressed in UC-nonprogressors, but not UC-progressors. Mir-155 has been implicated in the regulation of T-cell subsets, particularly Th17 cells that express IL-17. In situ hybridization using a mir-155 specific probe and IHC staining for IL-17 validate these biomarkers in situ within lamina propria lymphocytes.
Conclusions: We have identified a subset of miRNAs that are specifically misregulated in UC-nonprogressor and progressors that may prove useful as a biomarker panel to enhance early cancer detection and prevention in UC. Mir-155 is implicated in controlling the immune cell environment in UC. Its involvement as a biomarker has been validated by RT-PCR, in situ hybridization and immunohistochemistry for TH17 cells in nondysplastic rectal biopsies.

1832 Mutation Profiling of Bladder Cancer Using Ion Torrent Sequencing

EM Wojcik, AB Rosenfeld, MI Zillox, ML Quek, GA Barkan, X Gai. Loyola University, Maywood, IL.
Background: Urothelial carcinoma of the bladder (UC) is the second most common genitourinary malignancy in the United States. Current diagnostic tests are based on a specific biomarker or genetic alteration, and have modest sensitivity and specificity. We hypothesize that mutation profiles of known oncogenes and tumor suppressor genes collectively can distinguish different subgroups, therefore be used for accurate diagnosis, prognostic monitoring, and predicting treatment response.
Design: Histopathological examination of formalin-fixed, paraffin-embedded (FFPE) samples differentiated normal bladder tissue from tumor tissue (High grade UC, T2b). In a pilot study, DNA was isolated from pairs of UC and normal tissues of 5 patients using the AMBION Recovery all protocol. Genomic regions encompassing 739 known COSMIC mutations in 46 oncogene and tumor suppressor genes were amplified using Ion Torrent Ampliseq cancer panel protocol, which were then sequenced using the Ion Torrent Personal Genome Machine. An average base coverage depth of 570X across all target regions was achieved. Variant calls were made using the Ion Torrent Suite of software tools.
Results: We detected 7-40 genetic variants in each sample, with the majority being previously unknown somatic mutations. The overlap between the normal and cancerous tissue was less than 30% in each patient, suggesting the histologically normal tissues were possibly pre-cancerous. We found variants in exons, introns and the 3' UTR of genes that resulted in 52 silent, 83 missense and 5 nonsense coding changes. In addition, we detected 9 deletions resulting in frameshifts. Further analysis using this limited sample size suggested a positive correlation of the number of mutations with patient age. Between patients, we found the highest number of mutations in the APC, FGFR3, KDR and PDGFRA genes with few overlaps.
Conclusions: Our results revealed a large number of novel cancer mutations and confirmed 1) the highly heterogeneous nature of urothelial carcinoma, both within and between samples, 2) the presence of a large number of somatic mutations in the histologically normal surrounding tissues; 3) the lack of a common bladder cancer mutation in these oncogenes and tumor suppressor genes, and hence 4) the potential need of personalized genetic test for each patient. In addition, our preliminary results are in agreement with the hypothesis that accumulation of somatic mutations in the bladder cells as people age leads to pre-cancerous cells and eventually cancer.

1833 Whole Genome Analyses of Pancreatic Acinar Cell Carcinomas

LD Wood, Y Jiao, R Yonescu, JA Offerhaus, DS Klimstra, A Maitra, N Papadopoulos, KW Kinzler, B Vogelstein, RH Hruban. Johns Hopkins University, Baltimore, MD; University Medical Center Utrecht, Utrecht, Netherlands; Memorial Sloan-Kettering Cancer Center, New York, NY.
Background: Acinar cell carcinoma, a rare pancreatic carcinoma, is morphologically distinct from other pancreatic neoplasms, with unique clinical and immunohistochemical features. However, the genetic alterations underlying the development of acinar cell carcinoma have not yet been systematically explored.
Design: Twenty-three fresh frozen acinar cell carcinomas were macrodissected to achieve a neoplastic cellularity of >70%. Whole exome sequencing was performed on each carcinoma and matched normal tissue using next generation sequencing technology. The data were filtered for quality, and the alterations in the matched tumor and normal tissues were compared to identify tumor-specific somatic mutations. In addition, copy number arrays were performed on each tumor to identify large genomic alterations.
Results: Acinar cell carcinomas were characterized by striking genomic instability. While some carcinomas exhibited microsatellite instability, as evidenced by enrichment for single-base substitution mutations, other carcinomas showed marked chromosomal instability, with numerous large gains and losses throughout the genome. Chromosomal instability was validated by FISH which highlighted dramatic chromosomal alterations. Sequencing also revealed numerous somatic mutations. Acinar cell carcinomas contained somatic mutations in multiple components of the WNT signaling pathway (including *APC* and *CTNNB1*). Somatic mutations were also identified in druggable targets, including multiple hotspot mutations in *BRAF*. Infrequent somatic mutations were identified in genes known to be involved in pancreatic ductal adenocarcinoma, such as *TP53* and *SMAD4*, as well as genes involved in cystic neoplasms of the pancreas, such as *GNAS*. Acinar cell carcinomas lacked mutations in other genes implicated in pancreatic neoplasia, including *KRAS* and *ATRX/DAXX* (seen in pancreatic neuroendocrine tumors). In addition, acinar cell carcinomas contained somatic mutations in many genes not previously implicated in pancreatic neoplasia, indicating that these neoplasms are genetically distinct from the other neoplasms in the pancreas.
Conclusions: High-throughput molecular analyses of acinar cell carcinomas revealed that these carcinomas exhibit striking genomic instability. Although these carcinomas contain some genetic overlap with other pancreatic neoplasms, the results of this study indicate that acinar cell carcinomas are a genetically distinct neoplasm, possibly explaining their unique clinical behavior.

Pathobiology

1834 Detection of PML/RARA Fusion Protein in APL Using Proximity Ligation Assay as an Alternative to FISH Testing

J Bodo, JJ Lin, JP Maciejewski, AE Schade, ED Hsi. Institute of Pathology and Laboratory Medicine, Cleveland Clinic, Cleveland, OH; Taussig Cancer Institute, Cleveland Clinic, Cleveland, OH; Diagnostics Research/Development, Eli Lilly and Company, Indianapolis, IN.
Background: The presence of t(15,17)(q22;q12) resulting in *PML/RARA* fusion in acute promyeolocytic leukemia (APL) causes determines eligibility for immediate specific therapy. Currently, FISH and qPCR may be used to distinguish APL from other types of AML. We have developed a brightfield, slide-based method for the rapid *in situ* detection of the PML/RARA fusion protein using proximity ligation assay (PLA) and evaluated the correlation between PML/RARA fusion protein expression in APL and *PML/RARA* rearrangement.
Design: A total of 10 AML and APL cytospin samples with known *PML/RARA* FISH status were stained using PLA (OLINK Bioscience, Uppsala, Sweden) with PML and RARA specific antibodies. The principle of PLA is the recognition of target by two antibodies that can bring into proximity oligonucleotides that are conjugated to secondary antibodies. The oligos participate in ligation, creating a template for generating a large, tethered DNA molecule by amplification and detected with labeled hybridization probes, followed by brightfield detection.
Results: PLA was optimized with the NB-4 cell line (APL cell line with PML/RARA fusion protein) and SU-DHL-6 cell line (DLBCL cell line lacking PML/RARA fusion protein, but expressing normal PML and RARA). All 5 *PML/RARA* FISH positive APL cases were positive for PML/RARA expression by PLA. The majority of tumors cells were positive in *PML/RARA* rearranged cases (Figure 1). Importantly, there was no false positive staining among the 5 AML cases lacking t(15;17).
Conclusions: Early detection of PML/RARA is critical for directing appropriate therapy in APL. Our PLA specifically identified *PML/RARA*+ APL cases and can be performed and analyzed without specialized equipment. This is proof of principle that PLA can be used to detect clinically relevant fusion proteins with brightfield microscopy within a few hours.

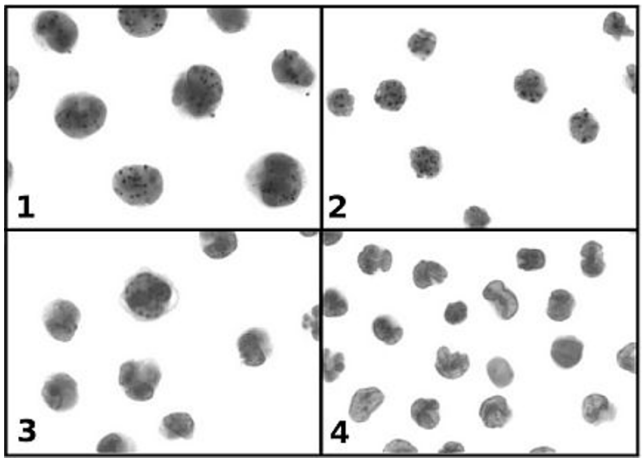

Figure 1. Detection of PML/RARA fusion protein expression by PLA. NB-4 (1) and SU-DHL-6 (3) cells served as positive and negative controls, respectively. Examples of PML/RARA+ APL (2) and PML/RARA- AML (4) samples are shown.

1835 Progesterone Induces NF-kB Activation through PI3K/Akt-2 Signal Pathway Which Regulates Focal Adhesion Kinase (FAK) in MCF-7 Breast Cancer

F Candanedo-Gonzalez, R Espinosa-Neira, S Villegas-Comonfort, N Serna Marquez, P Cortes-Reynosa, E Perez Salazar. Oncology Hospital, National Medical Center Century XXI, IMSS, Mexico City, Mexico; CINVESTAV-IPN, Mexico City, Mexico.
Background: Around 75% of breast tumors are positive for the progesterone receptor (PR). However, the signal transduction pathways activated by progesterone have not been studied in detail. The phosphatidyl inositol 3-kinase (PI3K) pathway plays an important role in breast cancer progression. Downstream of PI3K, Akt1 and Akt2, have opposing roles in breast cancer invasion migration, which lead to metastatic

dissemination in endocrine-treated breast cancer. Objective: To study the signal transduction pathways mediated by progesterone on MCF-7 breast cancer cells.
Design: MCF-7 breast cancer cells were cultured in DMEM, serum-starved for 12 h, and treated with inhibitors (Wortmannin, rapamicin, PP2) and/or progesterone (100 nM). FAK and Akt2 activation were analyzed by Western blotting using antibodies against phosphorylated specific amino acid residues. NFκB activation was analyzed by EMSA. Statistical analysis: Results are expressed as mean ± SD. Data were statistically analyzed using one-way ANOVA. Statistical probability of $p < 0.05$ was considered significant.
Results: Stimulation of MCF-7 cells with 100 nM progesterone promoted Akt2 activation through a PI3K dependent pathway, as well as FAK activation in a time-dependent manner. Moreover, progesterone induces NFκB activation in a time-dependent manner and it was dependent on PI3K, mTOR, Src and microtubule integrity.
Conclusions: Progesterone induces Akt2, FAK and NFκB activation through PI3K-dependent pathway in MCF-7 breast cancer cell. Our findings delineate a new signal transduction pathway mediated by progesterone in breast cancer cells. The understanding of these pathways will allow to offer new therapeutic options in the future.

1836 VEGFR1: Target for Anti-Angiogenic Therapy? An Immunohistochemical Study Highlighting Heterogeneity of Tumor-Associated Endothelial Cells

N D'Haene, F Hulet, J Allard, C Maris, C Decaestecker, I Salmon. Erasme Hospital, Université Libre de Bruxelles (ULB), Brussels, Belgium; Center for Microscopy and Molecular Imaging, ULB, Gosselies, Belgium.
Background: Research on tumour angiogenesis has mainly focused on vascular endothelial growth factor (VEGF) family and methods to block its actions. The fact that VEGFR1 could promote angiogenesis in pathological conditions makes it an attractive potential target. However, reports on the VEGFR1 expression in tumor-associated endothelial cells (EC) are limited. We decided to evaluate VEGFR1 expression in EC of human tissues.
Design: Immunohistochemical EC VEGFR1 expression was submitted to quantitative (computer-assisted microscopy) evaluation in a retrospective series of 130 normal and 785 malignant tumor tissues (including oral mucosa, esophagus, stomach, colon, thyroid, prostate and CNS). Results were related to clinical variables for colorectal carcinomas (CRC), glioblastomas (GBM) and thyroid carcinomas. EC VEGFR1 expression was also evaluated in a prospective series of 40 matched normal and tumor tissues (including lung, stomach, colon, liver and kidney).
Results: The data show that in normal tissue, EC expression of VEGFR1 was low. In contrast, a statistically significant increase of VEGFR1 expression was observed in EC of tumor tissues (Mann-Withney test: $p=0.006$ – Wilcoxon test for matched cases $p<10^{-6}$). However, a great heterogeneity was observed depending of tumor. The highest increases were observed for EC of oral squamous cell carcinomas and papillary thyroid carcinomas as compared to the normal counterpart ($p=0.009$ and $p=0.002$ respectively). For pT1-4N0-2M0-staged CRC (n=269), higher EC VEGFR1 expression was an independent prognostic factor in terms of metachronous metastasis ($p=0.03$). Altough the highest EC expressions of VEGFR1 was observed for some cases of GBM, EC VEGFR1 expression in GBM (n=181) was not associated with any prognostic values. Regarding thyroid carcinomas (n=42), higher EC VEGFR1 expression seems to be associated with lymph node metastasis ($p=0.08$), however this trend should be confirmed in a larger series.
Conclusions: This work illustrates the importance of studying target distribution. By its specific expression by tumor-associated EC VEGFR1 could be an interesting therapeutic target. However, expression heterogeneity across tumor types should be taken into account. Interestingly, higher EC VEGFR1 expression appears as being involved in CRC progression, suggesting that targeting EC VEGFR1 could offer novel opportunities for CRC treatment.

1837 High-Dimensional Mass Cytometry Analysis Reveals Differential STAT Activation in Cellular Subsets of Chronic Myelogenous Leukemia

J De, NP Shah, CT Ballentine, HT Maecker. Stanford University, Stanford, CA; University of California San Francisco, San Francisco, CA; MTFE Records, Oakland, CA.
Background: In chronic myelogenous leukemia (CML), the BCR-ABL translocation results in constitutive STAT5 activation. Despite their susceptibility to tyrosine kinase inhibitors (TKIs), STAT pathways have been implicated in therapy refractoriness. By blocking Bcl6, STAT5 enhances expression of IL6 which has been linked to myeloid expansion and blast crisis, and suppression of lymphoid differentiation. We sought to study cell-specific cytokine-potentiated effects on signaling events in CML by mass cytometry (MC), a powerful new approach to simultaneously quantify cell-specific effects of modulators on multiple oncogenic pathways.
Design: Fresh blood from a untreated 56y male patient with chronic phase CML was obtained from UCSF, and tested in parallel with a healthy donor sample. Aliquots of each were treated with IL3, IL6, IFNα, or no stimulus, for 15 min at 37C followed by surface staining prior to fixation, permeabilization, and intracellular staining. The panel of 27 markers included a series of metal-conjugated antibodies towards lineage-associated markers and phospho-specific epitopes within STAT5, STAT3, p38 MAP kinase, and PLCγ2; and total IκB kinase. Data from MC analysis was analyzed using high-dimensional analytical tools.
Results: Marked potentiated effect of IL3 on p-STAT5 was seen in cells derived from common myeloid progenitors (neutrophils, monocytes, and basophils); but not B- or T-lymphocytes in CML. Compared to normal B-cells, the B-cells in CML had higher baseline p-STAT5, but reduced IL3-STAT5 activity. The IL6-STAT3 pathway demonstrated higher activity in CML monocytes and CD4+ T-cells compared to normal counterparts. A minute IL3R-α expressing CD4+ T-cell subset showed STAT responses similar to myeloid progenitors. IL3-IκB was reduced in putative CD38- CD66+ myeloid blasts, suggestive of increased NFκB activity in this subset.
Conclusions: Findings of the present study offer novel insights into cell-specific oncogenic behavior and open avenues for further studies testing therapeutic role of inhibiting STAT and possibly NFκB in refractory CML. Reduced inducible STAT5 in CML B-cells raises questions regarding targetable STAT5 levels in B-lymphoid blast crisis and Ph+ acute lymphoblastic leukemia. Given the crucial role of IL6 in CML pathogenesis and its elevation secondary to Bcl6 repression, targeting Bcl6 while attractive due to its reactivation in TKI-refractory CML stem cells, must be critically evaluated.

1838 Nuclear Expression of PTEN in Endometrial Carcinoma

B Djordjevic, R Broaddus. University of Ottawa, Ottawa, ON, Canada; MD Anderson Cancer Center, Houston, TX.
Background: PTEN protein is a tumor suppressor which negatively regulates the PI3K–AKT signaling pathway via its cytoplasmic phosphatase function, and its loss is implicated in the pathogenesis of endometrial carcinoma (EC). Nuclear presence of the PTEN protein was recently found in cell lines to also have tumor suppressive activity via a mechanism independent of phosphatase activity. The purpose of this study was to characterize the nuclear vs. cytoplasmic expression of PTEN in a set of EC in which the *PTEN* mutation status is known.
Design: 154 EC cases consisting of 100 endometrioid and 54 non-endometrioid carcinomas were subjected to PTEN IHC analysis as well as to full-length *PTEN* gene sequencing to detect mutations. The PTEN antibody was previously validated on cancer cell lines. Cytoplasmic IHC staining was scored as positive (Cyto-pos:>90% of tumor with diffuse cytoplasmic staining), negative (Cyto-neg: 0% of tumor cells staining) and heterogeneous (Cyto-het: distinct positive and negative foci). Nuclear IHC staining was scored as positive (Nuclear-pos: >10% of tumor cells) or negative (Nuclear-neg: ≤ 10%).
Results:

	Cyto-neg, Nuclear-neg	Cyto-pos or het, Nuclear-neg	Cyto-pos or het, Nuclear-pos
ENDOMETRIOID n=100			
PTEN mutation	36	13	2
PTEN wild type	21	14	14
NON-ENDOMETRIOID n=54			
PTEN mutation	8	4	3
PTEN wild type	6	17	16

Nuclear PTEN expression, if present, was always observed concurrently within areas of cytoplasmic expression. In particular, no cases showed positive nuclear and negative cytoplasmic PTEN staining. Among ECs with a wild type PTEN, both endometrioid (50%) and non-endometrioid (48%) tumors showed similar frequencies of nuclear PTEN expression. In endometrioid ECs with a mutated *PTEN* and with cytoplasmic PTEN expression, a greater proportion (80%) of cases lacked nuclear expression compared to non-endometrioid ECs (20%).
Conclusions: Endometrioid ECs with a *PTEN* mutation and cytoplasmic PTEN expression preferentially lack nuclear staining and hence the nuclear tumor suppressor function of PTEN. Cytoplasmic expression in these cases may be secondary to retention of a non-functional PTEN protein. Interestingly, approximately 50% of *PTEN* wildtype EC with cytoplasmic PTEN protein expression, have loss of nuclear expression and thus loss of nuclear tumor suppressive function. In these tumors, cell proliferation may still be driven by the PI3K-AKT pathway through mutations in *PIK3CA* or other pathway members besides PTEN, or by upregulation of other signaling pathways.

1839 A Subset of Kaposi Sarcoma Cases Harbors Clonal Immunoglobulin Heavy Chain Gene Rearrangement: A Novel Finding Which Raises the Question of Transdifferentiation

JT Geyer, G Ballon, K Nie, YL Wang, E Cesarman. Weill Cornell Medical College, New York, NY.
Background: Kaposi sarcoma herpersvirus (KSHV/HHV-8) *vFLIP* oncoprotein expression in B cells produced a B cell-derived histiocytic/dendritic cell sarcoma (DCS) with monoclonal *IgH* gene rearrangement and downregulation of B cell-associated antigens (transdifferentiation), proving plasticity between B cell and macrophage/dendritic cell lineages in mice. Others achieved myeloid conversion of B cells *in vitro*. There are also reported cases of follicular lymphoma patients transdifferentiating into histiocytic/DCS and CLL patients with clonally related interdigitating DCS. Kaposi sarcoma (KS) is the most common neoplasm associated with KSHV. It is considered a tumor of endothelial origin. It usually contains a mixed infiltrate of histiocytes, lymphocytes and plasma cells (PCs). Monoclonality has been documented in some cases of KS. KSHV infects B lymphocytes, lymphatic and vascular endothelial cells. We hypothesized that infected B cells could transdifferentiate and be part of the spindle cell compartment of KS, with evidence of B cell monoclonality in a subset of cases.
Design: 21 patients with KS and 3 patients with other skin lesions were selected. Immunohistochemistry (IHC) for Pax-5, CD138, kappa, lambda, CD34, CD31, CD68, CD163 and KSHV was performed. PCR for *IgH* and *Jk* gene rearrangement was done. Cases with evidence of B-cell clonality were further manually laser microdisected (LCM) and PCR was performed to rule out contamination by B cells.
Results: IHC results showed that 10 KS patients had no B cells/PCs, while 11 had 1+ to 3+ B cells/PCs. Three of 17 cases (18%) with good quality DNA had a monoclonal *IgH* gene rearrangement. One patient had 3+ PCs; 2 had no B-cells/PCs. With LCM, cases 1 and 2 had a positive but polyclonal pattern. Case 3 had a persistent monoclonal band, similar to the original band.

Conclusions: We have identified 3 patients with KS and evidence of clonal *IgH* gene rearrangement in the spindle cells. In the absence of B cells, no rearrangements should be present. After LCM where only spindle cells were selected, two patients had a polyclonal B-cell pattern consistent with a B cell origin in at least some spindle cells, without showing monoclonality. One patient had a persistent monoclonal band with no evidence of B-cells or PCs by IHC and a pure population of spindle cells achieved with LCM. These results raise the possibility of occasional transdifferentiation in human cells infected with KSHV. This is a novel finding which sheds new light on the pathogenesis of KS.

1840 EZH2 Expands Breast Stem Cells by Activating Notch, Acting To Accelerate the Onset of Breast Cancer

ME Gonzalez, X Li, HM Moore, ML DuPrie, KA Toy, CG Kleer. University of Michigan, Ann Arbor, MI.

Background: EZH2 is a critical epigenetic regulator of cell type identity and has oncogenic functions in breast and other cancers, acting primarily as a transcriptional repressor through trimethylation of histone 3 at lysine 27 (H3K27me3). EZH2 upregulation signals increased risk for breast cancer when detected in benign breast biopsies. We hypothesized that EZH2 may promote breast cancer initiation through regulation of mammary stem cells.

Design: EZH2 was overexpressed in nontumorigenic breast cells using a Doxycycline-regulated or an adenoviral system. EZH2 was knocked down in breast cancer cell lines and cells derived from patients' tumors using specific shRNAs. The effect of EZH2 levels on mammary stem cells was investigated using mammosphere assay as well as flow cytometry (ALDH1+ and CD44+/CD24- assays). To study the effect of EZH2 on NOTCH1 transcriptional activity and promoter binding we employed reporter assays and chromatin immunoprecipitation (ChIP assays). The effect of EZH2 in tumor initiation was investigated using xenografts and genetic mammary specific EZH2 overexpression in MMTV-neu mice.

Results: EZH2 overexpression increased, while EZH2 knockdown (KD) decreased the number of mammospheres and the percentage of ALDH1+ and CD44+/CD24- cells in nontumorigenic and in breast cancer cells, respectively. NOTCH1 was one of the most significantly downregulated genes upon EZH2 KD in breast cancer cells. In nontumorigenic breast cells, EZH2 overexpression led to NOTCH1 mRNA and protein upregulation, and an increase in NOTCH1 transcriptional activity. Mechanistically, EZH2 binds to *NOTCH1* promoter (-1.2kb) independenly of the SET domain, but requires the HII domain. Consistent with EZH2-induced NOTCH1 activation, the binding of EZH2 to *NOTCH1* promoter was associated with increased H3K4me3 activating mark and with binding of RNA polymerase. Blockade of NOTCH signaling with GSI or NOTCH1 downregulation using siRNAs rescued the EZH2-mediated stem cell expansion in breast cells. Genetic EZH2 overexpression in MMTV-neu mice led to accelerated tumor initiation (log rank $p<0.005$).

Conclusions: EZH2 overexpression promotes breast cancer initiation *in vivo* by expanding the pool of functional breast stem cells via upregulation of NOTCH1. We uncover a novel role of EZH2 in activating, rather than repressing, NOTCH1 signaling through binding to *NOTCH1* promoter through the HII EZH2 domain. NOTCH1 is required for EZH2-mediated stem cell expansion in breast cancer. The new mechanism described herein may shed light into the tumor promoting effects of EZH2 in multiple solid tumors.

1841 Concordance for ERG and PTEN in Matched Primary and Metastatic Prostate Cancer: Further Evidence That PTEN Loss Occurs Subsequent to ERG Gene Fusion in Prostate Cancer

B Gumuskaya, B Gurel, JL Hicks, TL Lotan, A De Marzo. Johns Hopkins Medical Institutions, Baltimore, MD.

Background: Studies of the natural history of tumor initiation and progression are critical for understanding the molecular pathobiology of cancer. A recent study from our group has determined that while ERG expression by IHC tends to be homogeneous in an individual tumor nodule, PTEN loss is often heterogeneous suggesting that ERG rearrangement generally occurs prior to PTEN loss (Lab Invest, 92, Supp 1, 210A, 2012). To test this hypothesis further we used IHC to examine the rate of concordance between these markers in the index tumor from a radical prostatectomy (RRP) specimen and that of a corresponding metastatic lesion found in a pelvic lymph node at the time of RRP. In addition, we examined whether staining for each marker was homogeneous or heterogeneous in the primary and metastatic lesions.

Design: Two tissue microarray blocks were constructed from matched primary (index tumor) and metastatic carcinomas from pelvic lymph nodes from 63 patients that had undergone radical prostatectomy at The Johns Hopkins Hospital. The carcinoma focus with the largest volume and/or highest grade was selected as the index tumor.

Results: 62% (N=37/60) of primary and 60% (N=36/60) of metastatic tumors present on the TMAs were positive for ERG and none of the cases had heterogeneous staining. 44% (28/63) of primary and 40% (23/58) of the metastatic tumors showed PTEN loss. The fraction of cases showing heterogenous PTEN staining in the primary tumor was 13.3% (8/60) and for the metastatic tumors it was 3.7% (2/54). The proportion of cases that were concordant for staining for ERG in the primary and metastatic lesions was 98.3% (57/58) and for PTEN it was 84.2% (49/57), and these proportions were statistically significantly different ($P = 0.0073$, two sample test of proportions).

Conclusions: The finding of highly concordant ERG staining in the index and metastatic tumor is supportive of the hypothesis that the index tumor and the metastatic lesion are clonally related (as seen previously by Guo et al. Hum Pathol. 43:644-9, 2012). The decreased concordance between PTEN loss in the primary and metastatic lesions as compared to ERG, along with the heterogeneity of PTEN staining, provides additional support for the contention that PTEN loss occurs at a later stage than ERG rearrangement during the natural history of prostate cancer evolution.

1842 Galectin-3, STn and Tn: Expression Profile in Pancreatic Neoplasms and Gastrointestinal Stromal Tumors

K Jiang, C Cohen, SR Stowell, RD Cummings, MT Siddiqui. Emory University School of Medicine, Atlanta, GA.

Background: Dysregulated levels of glycan-binding proteins, especially Galectin-3, have been identified in a spectrum of malignancies. However, its contribution to the pathogenesis and progression of cancers awaits characterization. Aberrant expression of glycan antigens Tn and sialylated STn have also been implicated in tumors. However, the potential diagnostic utility of these molecules in pancreatic neoplasms and gastrointestinal stromal tumors (GIST) has not been characterized. This study aims to assess their expression and to determine their diagnostic utility in these neoplasms.

Design: Galectin-3, Tn and STn were evaluated immunohistochemically in fine needle aspiration (FNA) cell blocks (CB) from: 1) 46 pancreatic ductal adenocarcinoma (PDAC), 2) 8 non-neoplastic pancreas, 3) 5 pancreatic neuroendocrine neoplasms (PNEN), and 4) 13 GIST. Membranous and granular cytoplasmic labeling (3+ and >10% cells) was considered positive. The data were analyzed by statistical analysis.

Results: Forty-four, 43, and 41 of 46 PDAC CB demonstrated tumor-specific Galectin-3 (sensitivity 95.7%; specificity 87.5%), Tn (sensitivity 93.5%; specificity 87.5%), and STn positivity (sensitivity 89.1%; specificity 87.5%), respectively. Adjacent non-neoplastic tissue showed either negativity or minimal levels of Tn and STn. In contrast, only 12.5% (1/8) non-neoplastic pancreas showed focal 2+ Galectin-3, Tn, or STn signal ($p<0.001$). Importantly, no positivity for Galectin-3, Tn or STn was detected in PNEN and GIST studied.

	Gal-3 +++	Gal-3 -	Tn +++	Tn -	STn +++	STn -
PDAC (46)	44 (95.7%)	2 (4.3%)	43 (93.5%)	3 (6.5%)	41 (89.1%)	5 (10.9%)
Non-neoplastic pancreas (8)	1 (12.5%)	7 (87.5%)	1 (12.5%)	7 (87.5%)	1 (12.5%)	7 (87.5%)
Total (54)	45	9	44	10	42	12

P<0.001 for all 3 markers; Gal-3: Galectin-3

Type	Gal-3 +++	Gal-3 -	Tn +	Tn -	STn +	STn -
PNEN (5)	0 (0%)	5(100%)	0 (0%)	5(100%)	0 (0%)	5(100%)
GIST (13)	0 (0%)	13(100%)	0 (0%)	13(100%)	0 (0%)	13(100%)

Negativities in PNEN and GIST

Conclusions: Unique and significant expression of Galectin-3, Tn and STn is demonstrated in PDAC, with minimal to negative levels in adjacent non-tumor tissue and normal pancreas. This is in sharp contrast to their lack of immunoreactivity in PNEN and GIST. These data strongly suggest their crucial roles in the pathogenesis and diagnosis of PDAC, but not in PNEN and GIST. They can potentially be utilized in challenging cases to aid in diagnosis of PDAC.

1843 Expression of Cancer Testis (CT) Antigens in Thymus of the Fetus

AA Jungbluth, D Frosina, M Holz, S Gnjatic, GC Spagnoli, AM Mueller. Ludwig Institute for Cancer Research, New York, NY; University Hospital, Basel, Switzerland; University Hospital, Bonn, Germany.

Background: CT antigens such as NY-ESO-1, MAGE, GAGE, and CT7 are named after their characteristic pattern of expression, since they are found in various types of cancer and in normal adult tissues solely present in testicular germ cells. They are also present in fetal ovarian germ cells and occasionally in placenta. In cancer patients, some CT antigens are highly immunogenic and due to their limited expression in normal tissues, are used as vaccine targets for cancer immunotherapy. They also serve as markers of malignancy. Little is known about the biology of CT antigens and especially their role in the normal immune system. Consequently, here was analyzed the presence of CT antigens in a series of fetal thymic tissues.

Design: Archival thymus tissue from 40 fetuses (week 15-42) was available for analysis. IHC using the following mAbs (to the following CT antigens) were used: MA454 (MAGE-A1), 57B (MAGE-A4), E978 (NY-ESO-1), #26 (GAGE), CT7-33 (CT7), and CT10#5 (CT10).

Results: Expression of CT antigens in thymus was highly variable. NY-ESO-1 remained completely negative. MAGE-A1 was present in single cells of only three cases. CT7 and CT10 were present in 10 and 11 thymi respectively, both showing solely focal staining. GAGE and MAGE-A4 were most abundantly expressed: GAGE was present in 22/40 and MAGE-A4 in 27/40 tissues; both antigens displayed large groups of positive cells. For all tested antigens, immunopositive cells were restricted to the medulla and were exclusively epithelial cells. There was not predilection of any gestational age for any of the tested antigens.

Conclusions: The present study shows that -irrespective of fetal age- several CT antigens are consistently present in fetal thymus, albeit to a variable degree. Expression is restricted to thymus epithelial cells and ranges from a few cells to larger groups of cells; GAGE and MAGE-A4 are most abundantly present. Interestingly, there was no NY-ESO-1 expression in any of the tested thymi. These data complement serological data in cancer patients which show rare immune responses to those antigens, which were highly expressed in our series of thymus tissues. NY-ESO-1, however, is the most immunogenic antigen in cancer patients. The lack of NY-ESO-1 expression in fetal thymus could be the cause of lacking pre-existing immunotolerance to NY-ESO-1 rendering cancer patients more sensitive to the presence of NY-ESO-1 in cancer tissue and consequently to vaccine applications.

1844 Clinical Utility of ERG Immunohistochemistry as a Vascular Marker with Assessment of Lymphovascular Invasion

S Kim, HK Park, HY Jung, SD Lim, WY Kim, HS Han, TS Hwang, WS Kim. Konkuk University Medical Center, Seoul, Republic of Korea.

Background: ERG, member of the ETS family transcription factors is a highly specific vascular marker and the clinical utility of ERG immunohistochemistry (IHC) for assessing lymphovascular invasion (LVI) has not been studied yet. We investigated clinical utility of ERG immunohistochemistry (IHC) for assessing LVI relative to HE only or the previous vascular markers.

Design: In the first round review (FRR) of LVI, 15 cases of surgically resected colorectal cancers (CRCs) with lymph node and liver metastasis from the pathology archives were collected. HE stain and IHCs for ERG, CD31, and D2-40 were performed on each representative section for assessing LVI. First 6 pathologists independently evaluated LVI in HE only. Each combined HE & IHC slides were recirculated to reevaluate LVI. Finally consensus meeting was held and all participants reassessed LVI. After intensive discussion and education about assessing LVI in FRR, the second round review (SRR) of LVI with another 10 CRCs was performed. Results were analyzed by kappa(κ) statistics.

Results: In FRR, average κ values of HE only, CD31, D2-40, and ERG were 0.27, 0.55, 0.21, and 0.23 respectively. Agreement was moderate for CD31 IHC due to high negative rate (80%). Good agreement after consensus was observed for use of ERG IHC (κ=0.65) with high positive rate of LVI (80%). In SRR, better agreement with assessment of LVI using IHCs was observed relative to HE only ($p<0.01$).

Conclusions: We demonstrated a superiority of ERG IHC for the pathologists to recognize LVI relative to the histology only or use of the other markers. Our results prompt further validation study of its prognostic utility in various cancers and educational module with assessment of LVI.

1845 TGR5-Mediated NADPH Oxidase NOX5-S Expression Contributes to Bile Acid-Induced DNA Damage in Barrett's Esophageal Adenocarcinoma Cells

D Li, M Resnick, J Wands, W Cao. Rhode Island Hospital and the Alpert Medical School of Brown University, Providence, RI.

Background: Gastro-esophageal reflux disease complicated by Barrett's esophagus (BE) is a major risk factor for esophageal adenocarcinoma (EA). There is considerable data suggesting that bile acids may contribute to the pathogenesis of progression from BE to dysplasia and adenocarcinoma. However, the mechanisms whereby bile acid reflux may accelerate this progression are not fully understood. We have previously shown that bile acid-induced NOX5-S expression depends on activation of bile acid receptor TGR5. In this study we examined whether TGR5-mediated NOX5-S expression is involved in bile acid-induced DNA damage in a Barrett's EA cell line FLO.

Design: DNA damage was measured by using a Comet assay which is based on the ability of denatured cleaved DNA fragments to migrate out of the cell under the influence of an electric potential. It is quantitated by measuring the tail length, tail area and tail moment. The phosphorylation of histone H2AX was examined by Western blot analysis.

Results: Bile acid taurodeoxycholic acid (TDCA, 10^{-11}M, 24h) significantly increased tail length from 0.3±0.1 to 8.2±0.5 pixels, tail area from 15.5±5.3 to 272.4±16.6 pixels, and tail moment from 0.9±0.3 to 3.1±0.3, suggesting that TDCA increases DNA damage. To further confirm this result, the phosphorylation of histone H2AX, an indicator of double strand DNA break, was examined. TDCA markedly increased histone H2AX phosphorylation. TDCA-induced increase in tail length, tail area, tail moment and histone H2AX phosphorylation was significantly decreased by knockdown of NOX5-S with NOX5 siRNA. Conversely, overexpression of NOX5-S significantly increased tail length, tail area, tail moment and histone H2AX phosphorylation. Pre-treatment with diphenylene iodonium, an inhibitor of NOX, prevented the bile acid-induced increase in tail length, tail area and tail moment. In addition, TDCA-induced increase in tail length, tail area and tail moment was significantly decreased by knockdown of TGR5 with TGR5 siRNA, whereas overexpression of TGR5 with TGR5 plasmid significantly increased DNA damage.

Conclusions: Bile acid treatment causes DNA damage via activation of TGR5 and NOX5-S. It is possible that in Barrett's esophagus bile acid activates TGR5 and NOX5-S, and increases ROS production, which causes DNA damage, thereby contributing to the progression from BE to EA.

Supported by NIH NIDDK R01 DK080703.

1846 The RANK Pathway in Breast Cancer: Src Plays a Role!

R Li, T Nguyen, C Kragel, K Zhang, WE Grizzle, O Hameed, GP Siegal, S Wei. University of Alabama at Birmingham, Birmingham, AL.

Background: Receptor activator of nuclear factor κB (RANK) and its ligand, RANKL, are essential for mammary gland development. The molecules also play a key role in osteoclastogenesis and osteolytic bone metastasis. Previous studies suggested that RANKL expression was inversely correlated with the metastatic phenotype in breast cancer (BC), and RANK expression was a poor prognostic factor in BC with bone metastasis. Src, a nonreceptor tyrosine kinase overexpressed in 70-100% of BCs, plays a key role in several transduction pathways. The RANK cytoplasmic tail associates with Src, leading to activation of anti-apoptotic signaling. The aim of this study was to examine the expression of these molecules in BC and to investigate their potential roles in metastasis.

Design: Tissue microarrays (triplicate 1-mm cores/case), constructed from 62 primary BC cases with known metastasis and 10 control BC cases (no relapse for ≥ 8 years of follow up), were stained with RANKL, RANK and Src antibodies. The intensity and percentage of tumor cell staining were multiplied to determine an H-score.

Results: Neither RANKL or RANK expression was significantly different in BCs with and without metastasis, or associated with a bone metastatic phenotype in BCs with metastasis. Interestingly, a significantly lower level of RANKL and a significantly higher level of RANK were found in triple-negative (TN) BCs when compared to luminal BCs ($p<0.01$, $p<0.05$)), whereas expression levels of the two molecules in the HER2 subtype were between luminal BCs and TNBCs. Given that TNBCs reportedly have a higher predisposition for brain metastases, it is not surprised that expression of these molecules was significantly associated with a brain metastatic phenotype (both $p=0.01$). RANK expression was additionally associated with multiple organ metastases ($p<0.01$). Similar to RANK, Src expression was also significantly higher in TNBCs ($p<0.05$), BCs with brain metastases ($p<0.05$) and BCs with multiple organ metastases ($p<0.01$), but was not associated with a bone metastatic phenotype, a finding consistent with gene expression profiling. Further, a strong linear correlation was found between RANK and Src expression ($r=0.6$, $p<0.0001$).

Conclusions: Despite their high expression in bone, RANKL or RANK expression is not associated with BC bone metastasis. Rather, they differ significantly between molecular subtypes. The strong correlation of RANK and Src expression suggests that Src may be a downstream effector of RANK in BC cells. Thus, targeted therapy to these molecules may lead to success, especially in TNBCs, for which there are only limited effective treatment options.

1847 Common MicroRNA Biomarkers To Characterize Inflammatory Bowel Disease

J Lin, Z Zhao, NC Welker, Y Liu, X Zhang, J Zhang, Y Li, H-J Lee, MP Bronner. Indiana University School of Medicine, Indianapolis, IN; University of Utah, Salt Lake City, UT; Albany Medical Center, Albany, NY.

Background: The pathogenesis of idiopathic inflammatory bowel disease (IBD), either ulcerative colitis (UC) or Crohn disease (CD), is integrated from genetic, epigenetic, and environmental factors. The pathologic diagnosis of IBD can be challenging if the patient presents with fulminant colitis. MicroRNAs (miRNAs) are small, noncoding RNAs, which regulate the physiological processes by preventing protein synthesis through posttranscriptional suppression.

Design: This study examines whether common miRNA biomarkers of IBD can be identified and whether they might assist in diagnosing IBD. Illumina small RNA sequencing was performed on nondysplastic fresh-frozen colonic mucosa samples from patients with a diagnosis of IBD (10 UC and 9 CD) and from 18 patients with diverticular disease as "normal" controls.

Results: USeq software was used to identify 9 miRNAs with altered expression in both UC and CD (fold change, ≥2; false discovery rate, ≤0.10) compared to normal controls. Validation assays were performed using qRT-PCR on frozen tissue to confirm the altered expression of four of them (mir-31, mir-206, mir-424 and mir-146a) ($P<0.05$). Furthermore, the expression of these four microRNAs was evaluated on the formalin-fixed, paraffin-embedded tissue from cohorts of diverticular disease controls ($n=15$), UC ($n=35$), CD ($n=21$) and other diseases that mimic IBD including colonic infection ($n=12$) and ischemia ($n=12$). The expression of mir-31 was significantly increased in IBD groups compared to the control and the infections groups ($P<0.05$).

Conclusions: Our study indicates that mir-31 is commonly expressed in both UC and CD, regardless of the status of inflammation. Furthermore, mir-31 could be used as a valuable ancillary biomarker to diagnose IBD in either fresh-frozen tissue or routinely used formalin-fixed, paraffin-embedded tissue.

1848 Succinate Dehydrogenase Deficiency Is Associated with Decreased 5-Hydroxymethylcytosine Production in Gastrointestinal Stromal Tumors: Implications for Mechanisms of Tumorigenesis

EF Mason, JL Hornick. Brigham and Women's Hospital, Harvard Medical School, Boston, MA.

Background: Gastrointestinal stromal tumors (GISTs) usually harbor activating mutations in *KIT* or *PDGFRA*, which promote tumorigenesis through growth factor receptor signaling pathways. Around 15% of GISTs in adults and >90% in children lack such mutations ("wild-type" GISTs). Most gastric wild-type GISTs show loss of function of the Krebs cycle enzyme complex succinate dehydrogenase (SDH). The mechanism by which SDH deficiency drives tumorigenesis is unclear. Loss of SDH leads to succinate accumulation, which inhibits α-ketoglutarate-dependent dioxygenase enzymes, such as the TET family of DNA hydroxylases. TET proteins catalyze conversion of 5-methylcytosine to 5-hydroxymethylcytosine (5-hmc), required for subsequent DNA demethylation. Thus, TET-mediated 5-hmc production alters global DNA methylation patterns and thereby influences gene expression. In this study, we investigated 5-hmc levels in a cohort of genotyped GISTs to determine whether loss of SDH was associated with inhibition of TET activity.

Design: 30 genotyped GISTs were examined, including 10 SDH-deficient tumors (5 *SDHA* mutant; 1 *SDHB* mutant; 1 *SDHC* mutant; 3 unknown), 14 with *KIT* mutations (10 exon 11; 3 exon 9; 1 exon 17), and 6 with *PDGFRA* mutations (all exon 18). Immunohistochemistry was performed following antigen retrieval using a rabbit anti-5-hmc polyclonal antibody (1:10,000; Active Motif). Nuclear staining for 5-hmc in tumor cells was compared to endothelial cells and lymphocytes, which served as positive controls, and was scored as positive, weak (<50% intensity of controls), or negative.

Results: 5-hmc was negative in 9 of 10 (90%) SDH-deficient GISTs, 3 of 14 (21%) *KIT*-mutant GISTs (2 exon 11, 1 exon 17), and 1 of 6 (17%) *PDGFRA*-mutant GISTs. One SDH-deficient GIST showed weak staining for 5-hmc. All 3 *KIT* exon 9-mutant GISTs and 2 *PDGFRA*-mutant GISTs showed weak 5-hmc staining.

Conclusions: 5-hmc is absent in nearly all SDH-deficient GISTs. These findings suggest that SDH deficiency may promote tumorigenesis through accumulation of succinate and inhibition of dioxygenase enzymes. Inhibition of TET activity may, in turn, alter global DNA methylation in SDH-deficient tumors.

1849 STAT3 and STAT5a Are Potential Therapeutic Targets in Castration-Resistant Prostate Cancer

SK Mohanty, K Yagiz, B Cinar, MB Amin, D Luthringer, S Alkan. Cedars-Sinai Medical Center, Los Angeles, CA.

Background: Currently, there is no effective pharmacotherapy for metastatic castration-resistant prostate cancer (mCRPCa). The neoplastic cells develop resistance to androgen deprivation therapy within two to three years of therapy. The molecular mechanisms underlying this progression are not clearly defined, thus hindering rational-based drug design. Signal transducer and activator of transcription 3 (STAT3) and 5a/b (STAT5a/b) are suggested to play a role in promoting growth of high-grade hormone-resistant (HGR) PCa. Although molecular studies have shown expression of STAT3 and STAT5 on PCa cell lines, expression of STAT3 and STAT5 on tissue sections of HGRPCa are not studied. This study aims to determine possible role of STAT3 and STAT5a in HGRPCa.
Design: The anatomic pathology database was searched for HGRPCa after Institutional Review Board approval. We examined nuclear expression of STAT3 and STAT5a by immunohistochemistry (IHC) and the results were compared to fifteen cases of benign prostatic hypertrophy (BPH). In addition, we tested effects of STAT inhibitor (Pimozide) at 72 hours in androgen sensitive LNCaP and castration resistant LNCaP subline (C4-2) PCa cell models by assessing proliferative response to various concentrations (0, 5, 10 and 20 micromolar) in serum fed growth condition.
Results: Fifteen cases of HGRPCa and 15 cases of BPH were used for IHC assessment. Age ranged from 59 to 95 years (median = 81) in the former and 57 to 86 years (median = 68) in the latter category. The details of results of STAT3 and STAT5a immunostaining are illustrated in Table 1. Treatment with Pimozide showed a significant inhibition of LNCaP cell proliferation at 10 micromolar and of C4-2 cell proliferation at 20 micromolar concentration.

Categories	STAT3 (focal positive)	STAT3 (diffuse positive)	STAT3 (negative)	STAT5a (focal positive)	STAT5a (diffuse positive)	STAT5a (negative)
HGRPCa	8 (strong)	6 (strong)	1	4 (strong)	8 (strong)	3
BPH	7 (weak)	1 (strong)	7	10 (weak)	0	5

Conclusions: Our results demonstrate expression of STAT3 and STAT5a on tissue sections may potentially serve as a predictive marker of responsiveness to therapies targeting JAK/STAT pathway. Since JAK/STAT and androgen receptor (AR) signaling pathways functionally synergize in the neoplastic cells and may be involved in the progression of PCa, the inhibition of JAK/STAT alone or in combination with AR signaling may lead to a novel treatment modality for patients with CRPCa.

1850 General Grading System of Malignancies: High Grade Neoplasms Express Stem Cell-Like Phenotype

J Moorhead, J Gonzalez, A Blanes, SJ Diaz-Cano. King's College Hospital, London, England, United Kingdom; University of Malaga School of Medicine, Malaga, Spain.

Background: Grading is one of the most powerful variable of tumor prognosis, but is subjective, site dependent, and has little biologic support. We aim to identify the variables that reliably predict grade, testing stem cell features as potential discriminator.
Design: We analyzed primary and secondary growth patterns (tubulo-papillary, nested-trabecular, nodular-solid, diffuse), nuclear grade (including chromatin, nucleolus, pleomorphism and anisokaryosis), stromal reaction, and confluent necrosis in common malignancies: carcinomas (61 basal cell, 101 squamous cell, 163 adenocarcinomas, 30 urothelial, and 20 neuroendocrine), sarcomas (100), lymphomas (100) and melanomas (61). Tumors were graded according to the WHO classification (139 poorly differentiated). Representative samples were evaluated by quantitative RT-PCR and standard in situ techniques for stress-stem cell pathways (telomere PNA-FISH, TERT, TP53, ATF2, BMP4, PTCH1, FN1, CXCR3, MMP10, OCT4, SCF, MYC, JUN, and FOS), proliferation (Ki-67) and apoptosis (TUNEL assay). Appropriate controls were run. Fisher's exact tests and analysis of variance (significant if $P<0.05$) were used for comparison; significant variables were then selected for discriminant analysis with cross-validation for grading groups (well-moderate vs. poorly differentiated).
Results: The variables contributing most to the poorly differentiated neoplastic phenotype were the growth patterns, necrosis presence, hemorrhage, anisokaryosis, nucleolus, and Ki67 index. Stepwise discriminant analyses correctly classified 97% of cases (96% after cross validation). Telomerase expression and telomere positive cells (%) were the added variables for carcinoma grading. Telomerase/telomere indices directly correlated with the kinetic index, being significantly higher in high-grade malignancies with upregulation of TP53, ATF2, KITLG, CXCR3, MYC and FOS. The remaining markers revealed no statistically significant differences.
Conclusions: A reliable common grading system of malignancies must include a combined evaluation of growth pattern, confluent necrosis, nuclear and proliferation features. High-grade malignancies express stem-like phenotype with emphasis on stress (ATF2, FOS, TP53), survival (MYC, TERT) and microenvironment (CXCR3, KITLG) pathways.

1851 Mechanism of Ceramide-Induced Activation of Protein Phosphatase 2A

KK Narra, SA Summers. University of Utah, Salt Lake City, UT; Duke-NUS Graduate Medical School, Singapore, Singapore.

Background: Ceramide regulates cell metabolism, growth, and death. Inhibiting this sphingolipid **delays or prevents disease onset** in animal models of diabetes, cardiomyopathy, insulin resistance, atherosclerosis, and hepatic steatosis. Therapeutic strategies for treating these metabolic diseases will benefit from understanding the mechanism of action of ceramide. Among other molecular mechanisms, ceramide activates protein phosphatase 2A (PP2A), which dephosphorylates and inactivates Akt2 kinase, an insulin signaling intermediate. PP2A comprises of A (scaffolding), B (regulatory), and C (catalytic) subunits. The B subunit isoforms impart substrate and regulator specificity. *In vitro*, ceramide binds to inhibitor 2 of protein phosphatase 2A (I2PP2A), which then dissociates from PP2A thus activating the phosphatase. Here we show novel *in vivo* subcellular and molecular mechanisms by which ceramide regulates I2PP2A and PP2A.
Design: PP2A activity was measured in immunoprecipitates from H4iie (rat hepatoma) and U-87MG (human glioblastoma) cell cultures with *in vitro* and *in vivo* incubation with ceramide and also from dihydroceramide desaturase (DES1) knockout fibroblasts which completely lack ceramide. **Akt phosphorylation** was evaluated with knockdown of I2PP2A. PP2A activity and Akt phosphorylation were evaluated with **overexpression and knockdown** of select PP2A B subunit isoforms and with ceramide exposure. Using immunofluorescence, the effect of ceramide on **subcellular localization of I2PP2A** was studied. High fat diet (HFD) increases ceramide levels. Liver from **HFD-fed C57b/6 mice** treated with myriocin, a ceramide synthesis inhibitor, was evaluated for I2PP2A protein levels.
Results: In our experimental system designed to study allosteric mechanisms, ceramide did not activate PP2A by either *in vitro* or *in vivo* incubation; however, PP2A activity was reduced in DES1 knockout fibroblasts. Manipulation of expression of select B subunit isoforms did not affect ceramide-induced PP2A activity or Akt phosphorylation. Ceramide caused membrane localization of I2PP2A. Knocking down I2PP2A inhibited phosphorylation of Thr 308 but not Ser 473 residue of Akt. I2PP2A protein levels were decreased with HFD and were restored by reducing ceramide levels.
Conclusions: Ceramide-induced PP2A activation is not a direct allosteric mechanism. Ceramide causes subcellular translocation of I2PP2A thus dissociating the inhibitor from PP2A and activating the phosphatase. Ceramide causes long term regulation by decreasing I2PP2A protein expression.

1852 Specific Hemosiderin Deposition in the Spleen of TSOD Mice – A Unique Spontaneous Model Showing Obesity, Diabetes, Hyperlipidemia, and Steatohepatitis

T Nishida, K Tsuneyama, K Nomoto, S Hayashi, S Miwa, T Nakajima, Y Nakanishi, J Imura. University of Toyama, Toyama, Japan.

Background: Disturbance of iron metabolism was noted in patients with metabolic syndrome (MS). It is proposed that various proinflammatory and oxidant stress are associated with progress of the MS; however, the mechanism is still controversial. We recently reported a unique MS mice model, Tsumura-Suzuki-Obese-Diabetes (TSOD) mice, which develop obesity, type 2 diabetes, hyperlipidemia, and non-alcoholic steatohepatitis without any treatment. Interestingly, TSOD mice had significant hemosiderin deposition specifically in the spleen. It is thought that the state of iron metabolism, which is mainly regulated by the hepcidin-ferroportin system, was destroyed in the living body of TSOD mice. In this study, we investigated the mechanism of abnormal hemosiderin deposition in the spleen and the relationship to symptoms of MS.
Design: TSOD and Tsumura-Suzuki-Non-Obesity (TSNO) male mice, which were controls, were sacrificed at 8, 16, 24, and 32 weeks of age for histological and serum analysis. Spleen, liver, and visceral fat were removed and fixed in 10% formalin. The specimens were evaluated by hematoxylin-eosin staining, iron staining, and immunostaining such as IL-6 and 4-hydroxy-2-nonenal as a marker of oxidative stress. The serum levels of hepcidin and ferritin were measured by ELISA. Additional 4-, and 48-week-old TSOD and TSNO mice were sacrificed for gene expression analysis. The mRNA expression of ferroportin was investigated by real-time PCR analysis.
Results: In TSOD mice, excessive hemosiderin deposition was already observed at 8 weeks of age. The degree of hemosiderin deposition was worse until 32 weeks of age. The serum levels of hepcidin and ferritin of TSOD mice were higher than those of TSNO mice. Hemosiderin was located mainly inside macrophages of the spleen of the TSOD mice, and hemosiderin-laden macrophages expressed IL-6 intensely by immunostaining. In 48-week-old TSOD mice, expression of ferroportin, which has a role in exhausting iron from the cell, was lower than that of TSNO mice of the same age.
Conclusions: It was suggested that abnormal hemosiderin deposition in the spleen of TSOD mice was caused by underexpression of genes related to discharge iron from the macrophages such as ferroportin. On the other hand, hemosiderin-laden macrophages in the spleen showed overexpression of inflammatory cytokines such as IL-6. In this way, the macrophages that accumulated excessive iron may have the function of modifying various symptoms of MS. As a result, abnormal iron deposition may be indirectly related to pathologic progress in patients of MS.

1853 Association between Methylenetetrahydrofolate Reductase (MTHFR) Gene Variants and Hyperhomocysteinemia in United States Veterans

MM Pessarakli, RT Phan. Keck School of Medicine of USC, Los Angeles, CA; Veterans Affairs of Greater Los Angeles Healthcare System, Los Angeles, CA; David Geffen School of Medicine of UCLA, Los Angeles, CA.

Background: The MTHFR gene encodes 5,10-methylenetetrahydrofolate reductase (MTHFR), which regulates homocysteine metabolism. MTHFR gene variants such as C677T and A1298C may predispose to hyperhomocysteinemia - a risk factor for cardiovascular disease and arterial and venous thrombosis. Existing evidence for the relationship between MTHFR and hyperhomocysteinemia is, however, conflicting. This study investigates the association between MTHFR gene variants and hyperhomocysteinemia in a cohort of US veterans at the VA hospital in Los Angeles.
Design: This study is ongoing and includes 120 randomly selected cases from 01/2011-08/2012. Homocysteine level above 13.9 μmol/L is considered elevated. MTHFR is

genotyped by the eSensor platform and recorded for C677T variant as: CC (WT), CT (Het), TT (Hom); A1298C variant as: AA (WT), AV (Het), VV (Hom).

Results: 36 (30%) of 120 cases met selection criteria. Age range of patients is 31 to 90 years. Table 1 reports the MTHFR genotypes of the study population.

Table 1

MTHFR	CCAA	CTAA	TTAA	CCAV	CTAV	CCVV
No. (%)	9 (25)	10 (28)	4 (11)	7 (19)	5 (14)	1 (3)
Age (avg.)	63.5	55.3	56.75	60.7	64.6	65
Female	1(50)	0	0	1(50)	0	0
Male	8(23.5)	10(29.4)	4(11.8)	6(17.6)	5(14.7)	1(2.9)
Black	6(46.2)	1(7.7)	0	5(38.5)	0	1(7.7)
Caucasian	1(7.7)	5(38.5)	2(15.4)	2(15.4)	3(23)	0
Hispanic	0	1(100)	0	0	0	0
Other	2(22.2)	3(33.3)	2(22.2)	0	2(22.2)	0

15 (41.7%) of the 36 patients have elevated homocysteine. No association is observed between MTHFR C677T or A1298C and homocysteine level. The mean/median homocysteine levels among C677T genotype are CC(12.48/11.80), CT(14.4/13.14), TT(12.86/12.82); among A1298C are AA(13.19/12.56), AV(13.54/12.07), VV(16.19/16.19). Mean/median homocysteine levels for combined variants are shown in Table 2.

Table 2

MTHFR	CCAA	CTAA	TTAA	CCAV	CTAV	CCVV
Median	11.82	13.00	12.82	11.78	13.27	16.19
Mean	12.95	13.58	12.86	11.87	15.89	16.19

Conclusions: No association is found between MTHFR variants C677T or A1298C and elevated homocysteine. Compound heterozygous C677T/A1298C or homozygous C677T and hyperhomocysteinemia are also not correlated. The findings suggest that MTHFR variants are not reliable predictors of hyperhomocysteinemia among the US Veteran population. Additional data is expected at the USCAP Annual Meeting.

1854 *Gingko biloba:* A Potential Therapy for Lung Inflammation in Smokers

P Rastogi, J Marentette, J McHowat. St. Louis University - School of Medicine, St. Louis, MO.

Background: *Ginkgo biloba* has been used in traditional herbal medicine for several disorders. In this study we demonstrate that Gingkolides decrease inflammatory cell recruitment in the airways. Cigarette smoke causes small airway inflammation and inflammatory cell recruitment, resulting in widepsread damage which may progress to cancer. Platelet-activating factor (PAF) is a membrane phospholipid-derived metabolite formed by activation of calcium-independent phospholipase A_2 (iPLA2) and catabolized by PAF acetyl hydrolase (PAF-AH). PAF promotes trans-endothelial and trans-epithelial cell migration and we postulate that increased PAF production in the airways of smokers enhances inflammatory cell recruitment and exacerbates inflammation.

Design: Human small airways epithelial cells (HSAEC) were incubated with cigarette smoke extract (CSE) and PAF-AH activity and PAF accumulation measured. PAF production was inhibited with the $iPLA_2$ inhibitor bromoenol lactone (BEL). Next, we pretreated neutrophils with Gingkolide B, a PAF receptor blocker and measured their ability to adhere to the airway epithelial cell monolayers and transmigrate across them.

Results: Our experiments showed that PAF-AH activity decreased (3.8 $\pm$ 0.2 to 2.1 $\pm$ 0.3 nmol/mg protein/min, $p<0.05$, n=4) and PAF accumulation increased when airway epithelial cells were incubated with cigarette smoke extract (2277 $\pm$ 87 dpm to 5107 $\pm$ 203 dpm at 4 hours, $p<0.01$, n=6). PAF accumulation was blocked with BEL pretreatment. This suggests that increased PAF accumulation is a combination of increased synthesis ($iPLA_2$ activation) and decreased degradation (PAF-AH inhibition). We also observed a significant increase in neutrophil adherence to the airway eppithelial cell monolayers treated with cigarette smoke extract (15 $\pm$ 5 to 43 $\pm$ 6%, $p<0.01$, n=6). Cigarette smoke exposure also increased neutrophil transmigration (3-fold) across the cell monolayer in a basolateral to apical direction. Neutrophil adherence and transmigration was inhibited by pretreating PMN with Ginkgolide B to block the PAF receptor.

Conclusions: Taken together, our data demonstrate that increased accumulation of inflammatory cells in the airways of smokers depends on increased PAF production in the airway epithelium. In addition to smoking cessation, treatment with *Ginkgo biloba* may be a potential therapy to manage airway inflammation.

1855 Landscape of L1 Retrotransposon Expression in Human Carcinomas

N Rodic, R Sharma, KH Burns. Johns Hopkins Hospital, Baltimore, MD.

Background: Over a third of our genome by weight is comprised of repeated sequences known as long interspersed elements (L1s). L1s are retrotransposons that comprise of two proteins: open reading frame 1 (ORF1p), which coats nascent messanger L1 RNA; and ORF2p, which reverse transcribes and integrates L1 sequence. Because L1 ORF2p encoded endonuclease can introduce double stranded breaks into DNA, L1s may be considered as endogenous mutagens that may contribute to tumorigenesis in human cancer tissue.

Design: Using tissue microarray technology, we examined L1 ORF1p expression in a broad range of normal and malignant tissues. We devised a standard categorical scoring system for assaying L1 ORF1p levels of antibody staining to include: 0=Negative (<1% tumor cells are immunoreactive); 1+=Low level (<24% tumor cells are immunoreactive); 2+=Medium level (25%-74% tumor cells are immunoreactive); and 3+=High level (>74% tumor cells are immunoreactive). We finally evaluated L1 ORF1p expression using a binomial scoring system, where 1+,2+, and 3+ antibody staining were considered positive and no antibody staining was considered negative.

Results: Unlike unaffected human somatic tissue, which we found to be devoid of any detectable L1 ORF1p expression, we found that a large fraction of human malignant epithelial neoplasms are immunoreactive for L1 ORF1p antigen. L1 ORF1p was detected in all carcinomas examined including: lung and bronchus (41 out of 81 were immunoreactive); breast (9 out of 47); colorectal (19 out of 39); ovarian (23 out of 25); cervical (3 out of 22); pancreatic (9 out of 13); bladder (24 out of 44); endometrial (23 out of 30); salivary (19 out of 35); and esophageal carcinoma (9 out of 14). Because L1 expression has a potential to induce double stranded breaks, we reasoned that concomitant loss of p53 tumor suppressor gene, may contribute to clonal selection of L1 ORF1p expressing cancer cells. In fact, we find a strong tendency for the loss of p53 tumor suppressor gene in L1 ORF1p positive neoplasms in lung and bronchus carcinomas (n = 78, p-value = 0.0051); pancreatic carcinomas (n = 39, p-value = 0.00000047); and ovarian carcinomas (n = 25, p-value = 0.0000089).

Conclusions: We find that L1 ORF1p immunoreactivity is common to many carcinomas including pulmonary, pancreatic, and gynecologic (especially ovarian) malignancies. We further note that in many of these malignancies there is a tendency for the concomitant loss of p53 tumor suppressor gene in L1 ORF1p expressing tumors. Our study lays a foundation in understanding how L1 biology may contribute to human tumorigenesis.

1856 SIX1 Expression in Human Fetal Tissues

R Rong, L-P Wang, E Ruckdeschel, Z Bing. University of Pennsylvania, Philadelphia, PA; Upstate Medical University, Syracuse, NY.

Background: SIX1 is a key regulator of Epithelial-Mesenchymal transition (EMT), a cellular process that plays a major role in normal organ development and tumor progression. Congenital mutations of SIX1 gene have been identified in patients with Branchio-oto-renal syndrome, a development disorder characterized by hearing loss, branchial arch defects and renal anomalies. Overexpression of SIX1 correlates with adverse outcome in a variety of human tumors. In breast and colorectal cancer SIX1 has been shown to promote carcinogenesis and tumor progression through the induction of EMT. Although the expression of SIX1 during embryogenesis has been studied in mouse models in order to better understand its physiological role, the expression of SIX1 in human fetal tissue has not been systematically evaluated.

Design: We evaluated the expression of SIX1 in multiple fetal tissues including brain, heart, lung, kidney, adrenal gland, liver and small bowel. Twenty three archived human fetal tissue specimens were collected from the Dept. of Pathology at the University of Pennsylvania between 12/16/09 and 7/26/12. The gestational ages range from 15 to 21 weeks. Immunohistochemical staining for SIX1 was performed on paraffin-embedded tissue sections using rabbit polyclonal anti-SIX1 antibody.

Results: SIX1 is highly expressed in the subcapsular zone of the kidney. The strongest staining is noted in the metanephric mesenchyme surrounding the ureteric buds. As the metanephric mesenchyme undergoes mesenchymal to epithelial transition (the reverse process of EMT) and forms the renal vesicles, the staining of SIX1 is gradually reduced. Unlike previous findings in mouse models, there is minimal staining of SIX1 in the renal tubule epithelium. In the canalicular stage of fetal lung development, SIX1 shows strong staining in a subpopulation of bronchial tree epithelial cells, and moderate staining in terminal bronchiole, alveolar duct epithelium and scattered mesenchymal cells. In contrast, SIX1 has been shown to be specifically expressed in distal lung mesenchyme and epithelium in mouse embryos of similar gestational stage. In the remainder of the tissues examined, the staining of SIX1 is significantly weaker, the significance of which is unclear.

Conclusions: Our study demonstrates for the first time that SIX1 staining patterns differ between the human fetus and the mouse embryo of comparable gestational stage. We found that SIX1 is highly expressed in kidney and lung from second trimester human fetuses. Its expression is seen in both mesenchymal and epithelial cells.

1857 Enhancement of Cellular Tumorigenic Potential by Human Papilloma Virus and Epstein-Barr Virus Co-Infection

M Shi, R Jiang, O Ekshyyan, C-AO Nathan, L Fletcher, RS Scott. Louisiana State University Health Science Center, Shreveport, LA.

Background: Human Papilloma Virus (HPV) associated head and neck squamous cell carcinoma (SCC) are noted mostly in tonsil and base of tongue (BOT) and rarely in the rest of the oral cavity. The tonsil and BOT are histologically composed of lymphoid rich tissues that differentiate these two sites from all the other tissues in the oral cavity. The only other site in the head and neck with predominant lymphoid tissue is the nasopharynx, and carcinomas at this site are associated with Epstein-Barr virus (EBV). Examination of tonsillar and BOT SCC showed the presence of EBV/HPV co-infection in 25% and 50% of tumors, respectively.

Design: To determine the potential of EBV and HPV to synergize in the development of head and neck tumors, we developed an in vitro model to measure the tumorigenic potential of cell lines expressing various combinations of EBV and/or HPV. Normal oral keratinocytes were stably transfected with a plasmid carrying HPV16 E6 and E7 oncoproteins to mimic HPV infection followed by infection with a recombinant EBV strain. As control for selection, cognate vector lacking E6E7 or lacking EBV genes was transfected. EBV positivity and expression of E6 and E7 were confirmed by using reverse-transcription PCR with gene specific primers and western blotting. The expression of viral transcripts representative of the three EBV latency states was detected by RT-PCR, and the cell proliferation assay and cell invasion assay were conducted in these EBV/HPV cell lines.

Results: EBV-infected NOK displayed a type II latency profile that switched to a type III latency pattern with E6E7 expression. Cell proliferation was not significantly enhanced in NOK co-expressing E6E7 and EBV. However, co-expression of E6E7 and EBV cells significantly increased cellular invasiveness relative to parental, or E6E7 and EBV alone.

Conclusions: Our data indicated that co-infection of HPV and EBV not only influenced the EBV latency profile, but also enhanced cellular invasiveness, consistent with the metastatic nature of HNSCC tumors. Further studies are planned to evaluate the molecular basis for the enhanced tumorigenic potential by HPV/EBV co-infection using this in vitro model.

1858 Frequent Loss of PTEN and NM23H1 in Melanomas Harboring a BRAF V600E Mutation-Implications for Targeted Therapy

AN Snow, MM Milhem, AD Bossler, D Ma. University of Iowa Hospitals and Clinics, Iowa City, IA.

Background: *BRAF* is a member of the MAP kinase signaling pathway. *BRAF* V600E mutation is present in >50% of melanomas and associated with a more aggressive clinical course. Although BRAF V600E inhibitor, vemurafenib, has demonstrated improved progression-free and overall survival in patients with advanced disease, patients develop drug resistance and metastatic disease is rarely curable. Identification of other treatment targets is necessary. PTEN is a tumor suppressor in the phosphatidylinositol 3 Kinase (PI3K) pathway. Patients with PTEN loss in their tumors may benefit from combined therapy against PI3K pathway and vemurafenib or after vemurafenib failure. In this study, we evaluated the expression of PTEN and NM23H1, a metastatic suppressor, in BRAF wild type and V600E positive melanomas.

Design: Melanoma cases with (n=10) or without (n=12) BRAF V600E mutation were selected. BRAF mutation analysis was performed by Sanger sequencing. Immunohistochemical (IHC) stains for PTEN (Dako; clone 6H2.1, 1:100) and NM23H1 (Santa Cruz Biotechnology, clone: Nm301, 1:50) were performed on the same blocks used for molecular testing. The expression of PTEN and NM23H1 were scored using a 4-tier system. P: positive (≤90% of cells intensely positive); H: heterogeneous (regional positivity with >10% of cells negative); R: reduced (>10% of cells negative and decreased intensity of staining); and L: loss (≤1% of cells positive). Stromal cells served as positive controls.

Results: Decreased or absent expression of PTEN was observed in 41% of all cases examined. A higher frequency of reduced/loss of PTEN expression was seen in the BRAF V600E group (60%, n=10) versus BRAF wild-type tumors (25%, n=12). PTEN expression was also absent or reduced in 60% of cases with metastatic disease (n=10). 40% of BRAF V600E tumors showed absent or reduced NM23H staining. Four (all V600E positive) of 9 cases with PTEN loss/reduced expression also showed loss or reduced expression of NM23H1.

Correlation of PTEN and NM23 Staining

	PTEN			
NM23H1	P	H	R	L
P	10	0	2	2
H	0	1	0	0
R	1	1	3	1
L	0	0	0	1

Conclusions: A higher frequency of PTEN loss/reduced expression was observed in melanomas carrying V600E mutation. PTEN loss in melanomas especially in tumors harboring a BRAF V600E mutation may have implications for targeted therapy against the PI3K pathway in this subgroup of patients.

1859 Medullublastoma Expresses CD1d and Can Be Targeted for Immunotherapy with NKT Cells

L Song, D Liu, L Metelitsa. University of Texas Health Center at Houston, Houston, TX; Texas Children's Cancer Center, Houston, TX.

Background: Medulloblastoma (MB) is the most common brain tumor of childhood. Current therapies are not curative for a third of patients and have debilitating long-term toxicities.

Design: In this study we analyzed whether MB cells express CD1d, an antigen-presenting molecule for Natural Killer T (NKT) cells and could be targeted for direct NKT-cell cytotoxicity.

Results: We detected cell surface expression of CD1d in two of four human MB cell lines by flow cytometry and CD1d gene expression in the positive cell lines was confirmed by RT-PCR.

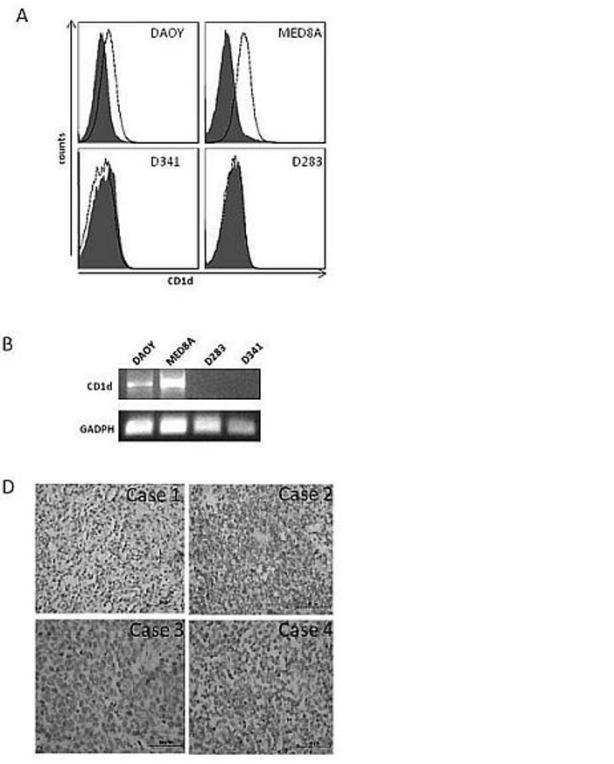

The immunohistochemical staining detected CD1d protein expression in 9 of 20 analyzed primary MB specimens. Nearly all tumor cells in the positive specimens expressed CD1d on the cell surface. In contrast, normal brain tissues were CD1d-negative except some vascular endothelial cells. Functional experiments demonstrated that CD1d-positive MB cells could effectively present synthetic type-I NKT cell ligands α-Galactosylceramide or 7DW8-5 as well as an endogenous ligand β-Glucosylceramide to activate NKT-cell cytokine production, proliferation, and cytotoxicity. Ligand-pulsed MB cells were highly sensitive to CD1d-dependent NKT-cell cytotoxicity *in vitro*, and intracranial injection of human NKT cells resulted in regression of established orthotropic human MB xenografts in NOD/SCID mice.

Figure 2

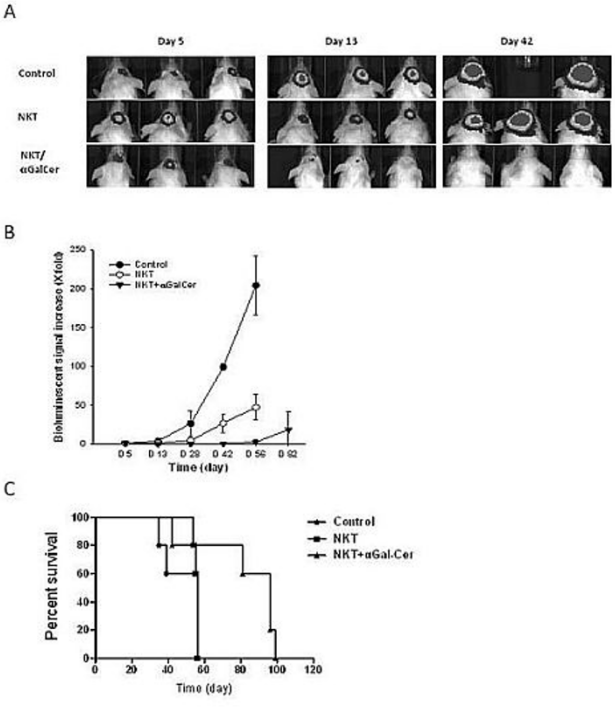

Importantly, both the numbers and functional properties of peripheral blood type-I NKT cells were preserved in MB patients to the levels similar to those in healthy individuals.

Conclusions: Therefore, CD1d is expressed on tumor cells in about half of MB patients and represents a novel target for immunotherapy of this brain tumor.

1860 Non-Destructive Microfluidic Cell-Based Assay for Determining Cell Deformability as a Function of Epithelial-to-Mesenchymal Transition

P Tavassoli, L Wang, S Park, H Ma, P Black. University of British Columbia, Vancouver, BC, Canada.

Background: The routine identification of circulating tumor cells (CTC) is based on cell surface expression of epithelial markers in the cancer cells. It is likely, however, that a subset of the most invasive CTC has lost expression of these epithelial markers in the process of epithelial-to-mesenchymal transition (EMT), a critical process that enables cells to detach from their primary site of growth, to invade and to metastasize. We have therefore developed a microfluidic device for the identification of CTC based on cell deformability. Here we aim to demonstrate that cell deformability depends on EMT status in bladder cancer cells.

Design: We have established a microfluidic technique for measuring the deformability of single cells. Cells are infused into a microfluidic channel and through a narrowing that requires cell deformation for passage. Using precisely controlled pressure, the cortical tension is determined by the liquid-drop model.

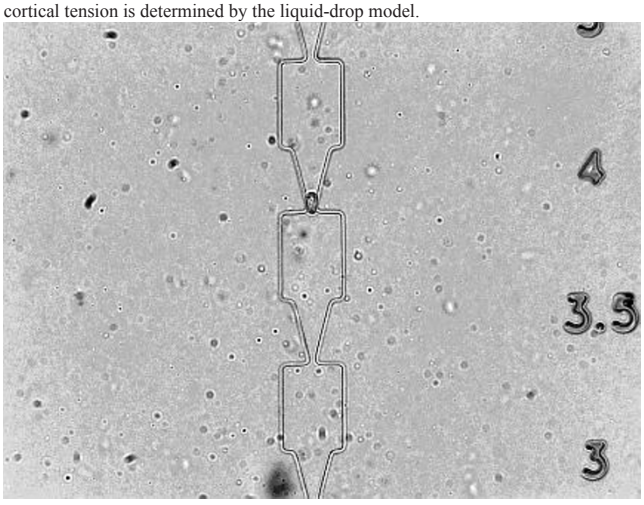

Zeb-1, a mediator of mesenchymal differentiation, was silenced in the highly invasive and mesenchymal cell line UC-13, while E-cadherin, the maker of epithelial differentiation, was silenced in UC-1. Differences in cortical tension and in invasive ability (matrigel invasion assay) were compared between these cells and the controls.

Results: UC-13 cells were less invasive after silencing of zeb1, and the mean cortical tension increased from 490 pN/µm to 837 pN/µm, representing a 1.7-fold increase in stiffness. Similarly, UC-1 cells were more invasive after silencing of E-cadherin, and the mean cortical tension decreased from 1198 pN/µm to 774 pN/µm, representing a 1.5-fold decrease in stiffness.

Conclusions: The non-destructive microfluidic cell-based assay enables us to measure the cortical tension of a variety of cells. We were able to demonstrate that cortical tension was inversely related to invasiveness of a bladder cancer cells, and both were dependent on EMT status. We therefore believe that EMT status will influence passage of CTC through our microfluidic cell sorting device, and aim to demonstrate this in ongoing work. This could be also potentially be used as a complementary test in for clinical cytology, especially in difficult samples such as urine cytology.

1861 *cMET* Mutations, Co-Mutations, and Survival Outcome

M Zenali, Z Liu, Z Zuo, R Broaddus. University of Vermont, Burlington, VT; University of Texas MD Anderson Cancer Center, Houston, TX.

Background: Proto-oncogene *cMET* and its ligand, HGF, are involved in survival & motility. Both mutation & overexpression of cMET gene have been found associated with driving tumorigenesis. There is also emerging evidence that some *cMET* mutations may be genetic polymorphisms. This study summarizes types of *cMET* mutations and rate of comutations with other genes in different tumors, including metastatic colorectal cancer (mCRC).

Design: We reviewed 1500 cases with panel mutation test (13 genes including *KRAS*, *BRAF*, *EGFR* and *cMET*), 47 cases had cMET mutations. In this group, SNPs, their distribution in tumor types, and incidence of comutations with other genes were recorded. mCRC was the largest tumor category harboring only *cMET* mutation. Survival outcome was determined for mCRCs with only cMET mutation (n=14) versus mCRC with no mutations (n=24).

Results: *cMET* point mutations were at five codons: 66 % N375S; 21% T1010I, and remaining: R988C & Y1248H & Y1253D. 50% of tumors with *cMET* mutation had mutation of at least one other gene in the panel. None of the cases with *cMET* mutation had amplification by FISH. Survival of the CRC patients with only *cMET* mutation was better than those without *cMET* mutation,not significant (p=0.057). Table 1 & figure 1.

cMET mutations & co-mutations

Tumor	cMET Mutation	Secondary Mutations
Colorectal Adeno	N375S, R988C, T1010I, Y1248H, Y1253D	P53, KRAS, PI3K
Melanoma	N375S, T1010I	NRAS, BRAF
Lung Adeno	N375S	EGFR, KRAS
Thyroid Ca.	N375S, T1010I	P53, BRAF, PI3K
Ovarian Ca.	N375S, T1010I	P53
Breast Ductal Ca.	N375S	PI3K
SCC of H&N	N375S, R988C, T1010I	PI3K
Prostatic Adeno	N375S	P53

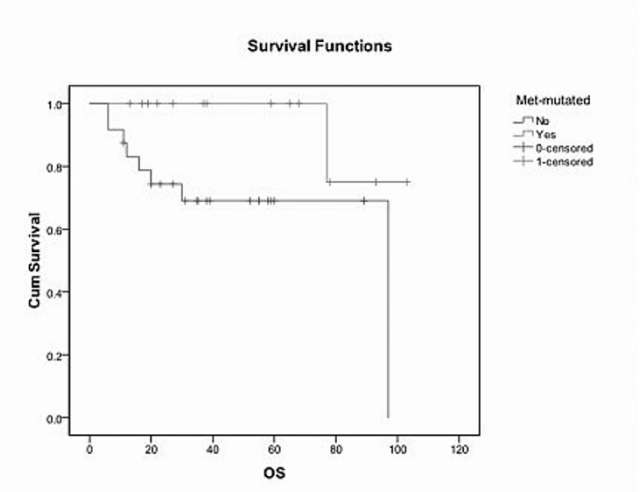

Conclusions: Incidence of comutations in tumors with *cMET* mutation is 50%, indicating a high probability of escape pathways in tumors harboring these mutations; this should be considered when therapeutically targeting *cMET*. Outcome in mCRC was not adversely affected by *cMET* mutation when excluding cases with comutations, suggesting that these may represent polymorphisms. A larger study is needed to further assess this concept.

1862 Loss of Heterozygosity (LOH) at 17p13 and 22q13 Is Associated with Metastasis and Shared by Breast and Thyroid Carcinomas

B Zhu, SD Finkelstein, JF Silverman, SM Rohan, X Lin. Northwestern University, Chicago, IL; RedPath Integrated Pathology, Inc., Chicago, IL; Allegheny General Hospital, Chicago, IL.

Background: Our previous studies have revealed that LOHs at a few specific chromosomal loci are involved in metastasis of breast ductal carcinoma (BDC) and papillary thyroid carcinoma (PTC). In this study, we compared the patterns of LOH involved in metastasis of BDC and PTC.

Design: We retrieved 14 BDC cases with known metastasis and 19 BDC cases without metastasis as well as 12 PTC cases with metastasis and 14 cases without metastasis. Analysis of 17 polymorphic microsatellite repeat markers (PMRM) targeting 1p34-36, 3p24-26, 5q23, 9p21, 10q23, 17p13, 17q12, 17q21, 21q22, and 22q13 was performed on DNA isolated from primary tumors.

Results: See Table 1 and 2

Table 1. LOHs in BDCs with or without metastasis.

Chromosome	PMRM	+ Metastasis*	- Metastasis*	P Value
1p34-36	D1S-1	4/9	2/15	0.039
	D1S-2	3/11	4/15	
3p24-26	D3S-1	6/12	3/13	
	D3S-2	6/10	2/11	
5q23	D5S-1	3/11	3/14	
	D5S-2	1/10	2/14	
9p21	D9S-1	5/10	3/17	
	D9S-2	5/11	4/16	
10q23	D10S-1	3/11	5/14	
	D10S-2	3/10	1/13	
17p13	D17S-1	5/11	3/15	
	D17S-2	4/11	1/13	0.014
17q12	D17S-3	4/8		
	D17S-4	3/8		
17q21	D17S-5	5/11	7/13	
21q22	D21S-1	3/11	1/12	0.036
22q13	D22S-1	5/11	1/11	

Yates' correction test. Cases with mutation/cases with informative markers.

Table 2. LOHs in PTCs with or without metastasis.

Chromosome	+ Metastasis	- Metastasis	P Value
1p36	7/12	5/14	
3p24	2/12	4/14	
3p12	0/12	3/114	
7p31	0/12	2/14	
9p21	6/12	8/14	
10q23	6/12	3/14	0.017
17p13	3/12	1/14	0.003
17q21	4/12	1/14	< 0.001
18q21	1/12	3/14	
21q22	3/12	3/14	
22q13	6/12	3/14	0.017

Yates' correction test.

Conclusions: 1. LOH at 1p34-36, 17p13 and 22q13 is significantly more common in BDC with metastasis compared to BDC without metastasis.
2. LOH at 10q23, 17p13, 17q21, and 22q13 is significantly more common in PTC with metastasis compared to PTC without metastasis.
3. LOH at 17p13 and 22q13 is shared by both BDC and PTC with metastasis, whereas LOH at 1p34-36 in BDC and LOHs at 10q23 and 17q21 is not shared.
4. Therefore, our results suggest that BDC and PTC share the same metastatic mechanisms that involve LOH at 17p13 and 22q13. The LOH signature may be clinically useful to better predict which carcinomas (breast and thyroid) might metastasize. More detailed studies to identified genes in these shared regions of LOH may provide insight into molecular mechanism of metastasis in these two tumor types.

Pediatrics

1863 Epithelioid Rhabdomyosarcomas: A Clinicopathologic and Molecular Study

R Alaggio, A Zin, A Rosolen, P Dall'Igna, G Bisogno, R Bertorelle. University of Padova, Padua, Italy; University Hospital Padova, Padua, Italy; Padua Hospital, University of Padua, Padua, Italy.

Background: Rhabdomyosarcoma (RMS), the most common pediatric soft tissue sarcoma is currently classified in 2 principal subtypes: embryonal (ERMS) characterized by variable genetic alterations including *TP53*, *RB1* and *RAS* mutations; alveolar RMS (ARMS), harbouring a gene fusion between *PAX3* or *PAX7* and *FOXO1*, with an aggressive clinical behaviour. Epithelioid RMS is a morphologic variant of RMS recently described in adults.

Design: 150 ARMS enrolled in Italian therapeutic protocols were reviewed in order to identify tumors with features of Epithelioid RMS and investigate their molecular features. Immunostainings (muscle specific actin, Desmin, Myogenin, AP-2β, EMA, cytokeratins, INI-1), reverse-transcriptase polymerase chain reaction (RT-PCR) assays to detect *MyoD1*, *myogenin*, and *PAX3/7-FOXO1* transcripts were performed. DNA sequencing of *TP53* was performed by capillary automated sequencer; *RB1* allelic imbalance (gain or loss) and homozygous deletion were analyzed by quantitative real-time PCR.

Results: Five Epithelioid RMS were identified. Clinical features are summarized in the table 1. Histology showed sheets of large cells without rhabdomyoblastic differentiation or anaplasia in 3 and prominent rhabdoid cells in 2; Necrosis in 4, often with a geographic pattern. Immunostainings showed: positive staining for INI, Desmin and Myogenin (scattered cells in 4, 70% in 1); EMA and MNF116 were positive in 2, AP-2β constantly negative. All tumors lacked *PAX/FOXO1* transcripts. *RB1* and *TP53* were wild type in 4 and 3 cases respectively, with mutation at R273H codon in 1.

Table 1

Case	Age/sex	Size	Site	Lymph-node Metastasis	Follow-up
1	9y/M	u*	HN-PM**	N1	ANED (8yr)
2	6y/M	3.3	HN-PM	N0	ANED (10yr)
3	13y/F	4	arm	N0	ANED (8yr)
4	11y/F	u**	arm	N0	u
5	8y/M	8.3	orbit	N0	ANED (4yr)

*unknown, **HN-PM head/neck parameningeal

Conclusions: RMS with epithelioid morphology rarely occurs in children. Lack of ARMS translocations, weak staining for myogenin and negative AP-2β suggest a potential relationship with ERMS, inline with by *TP53* mutation found in one case and by the favourable clinical course in the 3 patients with available follow-up.

1864 Pediatric Anaplastic Ependymoma: Morphoproteomics and Biomedical Analytics Identify Hypoxia Pathway Signaling and Provide Targeted Therapeutic Options

AQ Al-Ibraheemi, MF McGuire, RE Brown. UT Health-Medical School, Houston, TX.

Background: Relapsed, anaplastic ependymoma carries a poor prognosis, eventuating in death in approximately 90% of patients. Such tumors are largely chemoradioresistant. New therapeutic strategies will require defining the biology of anaplastic ependymoma. *Objective:* To profile pediatric anaplastic ependymomas using morphoproteomic techniques in an effort to identify pathogenetic commonalities amenable to therapeutic intervention and to employ biomedical analytics to translate such findings into targeted therapies. *Study Population: S*ix (6) pediatric patients (ages 3 to 10 years)with recurrent/progressive anaplastic ependymoma were included in this IRB approved study using morphoproteomic analysis.

Design: Morphoproteomics and biomedical analytics. Representative sections from formalin-fixed, paraffin-embedded sections of histopathologically proven cases of anaplastic ependymoma were received for morphoproteomic analysis.

Results: Hypoxia-inducible factor (HIF)-1 alpha expression with nuclear translocation was identified in four out of six tumors and showed correlative expression of:phosphorylated (p)insulin-like growth factor receptor; p-mammalian target of rapamycin (mTOR)[Ser2448] with nuclear translocation (favoring mTORC2); cyclo-oxygenase (COX)-2; p-p38 mitogen-activated protein kinase (MAPK)[Thr180/Tyr182]; secreted protein acidic and rich in cysteine (SPARC);and hypoxia/stemness markers to include CD133 and nestin.These coincided with the presence of ischemic-type coagulative necrosis in the same four cases. Biomedical analytics were then applied to the morphoproteomic analysis data. For each case, a scored profile was computed and used to generate the most likely biological pathway network model. The models revealed interactions with therapeutic agents that modulate hypoxia pathways including metformin, a histone deacetylase inhibitor (valporic acid), melatonin, celecoxib and doxorubicin

Conclusions: The application of morphoproteomics to recurrent/progressive anaplastic ependymoma cases reveals protein correlates of hypoxia pathway signaling which also accord with coagulative type necrosis in 4 out of 6 cases. This represents an adaptive pathway in such tumors to allow the emergence of chemoradioresistant populations and recurrent disease. Morphoproteomic analysis and biomedical analytics provide therapeutic options designed to target this adaptive pathway in cases in which the hypoxia pathway is identified.

1865 Correlation of Prenatal Diagnosis and Pathology Findings Following Dilation and Evacuation for Fetal Anomalies

CA Boecking, EA Drey, WE Finkbeiner. UCSF, San Francisco, CA.

Background: While pathology examinations are generally recognized as the "gold standard" for confirming clinical diagnoses, D&E procedures typically provide fragmented and/or incomplete specimens making clinical-pathological correlations difficult, imperfect or impossible. However, careful examination of fragmented fetal specimens is valuable and may confirm, supplement or correct diagnoses. In this study, we correlated pathology findings with prenatal diagnoses in D&E specimens.

Design: Clinical and pathology findings in 200 D&E specimens were correlated. Termination of pregnancy was based on abnormal karyotype in 90 cases and abnormal ultrasound examination in 110 cases. The pathology findings, sometimes multiple per individual case, were categorized into 1 of 4 groups (musculoskeletal, cardiac, genitourinary, or central nervous system [CNS]). Cases with multiple defects were also assigned to an additional category, Multiple Anomalies (MA).

Results: Ninety chromosomal abnormalities included trisomy 21 (48), trisomy 18 (23), trisomy 13 (8), and others (11). 51 (57%) of these cases showed at least one abnormality on pathology examination. In 110 cases where ultrasound led to D&E, at least one anomaly was confirmed in 76 (69%) specimens. In 22 of 54 cases of musculoskeletal anomalies, pathology examination confirmed the diagnosis. There were 15 cases with presumed cardiac defects; however, intact hearts were present in only 10 specimens. In these, examinations confirmed ultrasound findings in 6 and altered them in 4. Genitourinary anomalies were confirmed in 22 of 23 cases, with complete agreement in 14. Evaluating for CNS pathology proved challenging due to disruption from the D&E procedure. However, in 34 cases with ultrasound findings—anencephaly (22), encephalocele (4) and spina bifida (8)—the clinical diagnosis was confirmed in 53%. Since fetal anomalies are often complex and involve numerous organs, we also determined how often examinations could identify multiple abnormalities in a single case. Thus, in 68 MA specimens, abnormalities were identified in 48 with complete correlation in 8, partial correlation in 32, and 8 in which defects were incorrectly identified on ultrasound. Taking all categories into account, pathology studies yielded additional diagnostic findings in 21% of cases.

Conclusions: In a substantial number of cases, examination of fragmented fetuses corrects or refines prenatal diagnoses aiding subsequent genetic counseling.

1866 Recurrent *NCOA2* Gene Rearrangements in Congenital/Infantile Spindle Cell Rhabdomyosarcoma

JM Mosquera, A Sboner, L Zhang, N Kitabayashi, C-L Chen, YS Sung, M Edelman, MA Rubin, CR Antonescu. Weill Medical College of Cornell University, New York, NY; Memorial Sloan-Kettering Cancer Center, New York, NY; North Shore LIJ Health System, Flushing, NY.

Background: Spindle cell rhabdomyosarcoma (RMS) is a rare form of RMS with different clinical characteristics and behavior between children and adult patients. Its genetic hallmark remains unknown and it is debatable if there is a pathogenetic relationship between the spindle cell and the so-called sclerosing RMS.

Design: We studied two pediatric and one adult spindle cell RMS by next generation RNA sequencing. Data was analyzed using FusionSeq, a modular computational tool for gene fusion discovery. Additional 14 spindle cell RMS (from 8 children and 6 adults) and 4 sclerosing RMS (from 2 children and 2 adults) were screened by FISH.

Results: *SRF-NCOA2* gene fusion was detected in a spindle cell RMS from a posterior neck in a 7 month-old child. The fusion matched the tumor karyotype and was further confirmed by FISH and RT-PCR, which showed fusion of *SRF* exon 6 to *NCOA2* exon 12. *NCOA2* rearrangements were identified in 2 additional spindle cell RMS from a 3 month-old and a 4 week-old child, both arising in the chest wall. In the latter tumor, *TEAD1* was identified by rapid amplification of cDNA ends (RACE) to be the *NCOA2* gene fusion partner. All others were negative for *NCOA2* rearrangement.

Conclusions: Despite similar histomorphology in adults and young children, these results suggest that spindle cell RMS is a heterogeneous disease genetically as well as clinically. Our findings also support a relationship between *NCOA2*-rearranged spindle cell RMS occurring in young childhood and the so-called congenital RMS, which often displays rearrangements at 8q13 locus *(NCOA2)*.